Research on Chemical Intermediates (2023) 49:717–740
https://doi.org/10.1007/s11164-022-04884-6

Alginate-based foam filled with nano-zeolite for effective adsorptive removal of methylene blue from water: performance and effect of operating conditions

Maryam Kanani[1] · **Vahid Javanbakht**[1]

Received: 31 July 2022 / Accepted: 14 November 2022 / Published online: 5 December 2022

Abstract

One of the most toxic pollutants in the wastewater as a consequence of industrial activities is water-soluble dyes, which needed to be removed. In this study, a novel eco-friendly alginate-based foam adsorbent induced by ZSM-5 zeolite was prepared via simple freeze-drying and post-cross-linking method, characterized using different analyzes, and then used to remove methylene blue from aqueous solutions. Kinetics, isotherm, thermodynamics, mechanisms, contact angle and swelling investigation, regeneration, binary system experiments, and the parameters affecting the dye removal were investigated. The findings obtained from the batch adsorption process indicated that the adsorption of methylene blue using synthetic adsorbents has good conformity with conventional kinetic and isotherm models and the kinetics and isotherm are adjusted with the pseudo-second-order and the Temkin models, respectively. The adsorbent represented effective adsorptive removal of methylene blue with maximum efficiency of 97% and 4.57 mg/g adsorption capacity. With the increase in pH, concentration, and zeolite content in the foam, better adsorption performance was observed. Maximum dye adsorption was obtained in dye solution with 10 mg/L concentration, pH of 11, 25 °C, and adsorbent with 4 wt% zeolite content. The prepared adsorbents presented remarkable chemical stability and were readily recyclable with floatability in the aqueous solution.

Keywords Alginate foam · ZSM-5 nano-zeolite · Dye removal · Kinetics · Isotherm · Thermodynamics

✉ Vahid Javanbakht
javanbakht@jdeihe.ac.ir

[1] ACECR Institute of Higher Education (Isfahan Branch), Isfahan 84175-443, Iran

Introduction

Removal of the wastes from aquatic systems is an imperative issue from both human health and ecological perspectives [1]. Industrial dye effluents have turned into one of the most important pollutants in ecosystems. The effluents from textile, leather, printing, tanning, resin, plastic, paper, food, and cosmetics industries are the major sources of dyed wastewater [2, 3]. Methylene blue dye a highly stable cationic dye is one of the dyes that are used in dyeing cotton, wool, and silk. Inhaling this compound can cause respiratory distress and cause permanent damage to the eyes of humans and animals, local burns, nausea, vomiting, increased sweating, and mental disorders [4–6]. This dye affects the environment and damages the ecosystem, as its presence in the water prevents light from reaching the aquatic organisms and disrupts their life. Hence, its purification from water is very important [7]. Among the dye removal methods such as electrolysis, catalytic reduction, photocatalysis, membrane separation, chemical oxidation, and particularly adsorption, adsorption is an efficient and effective process because of its low cost, ease of use, and high efficiency [8–10]. Zeolites are the key microporous adsorbents and are considered selective adsorbents and contain ion exchange properties. Zeolite-based materials are quite diverse and used as ion exchange resins and adsorbents for wastewater treatment [11–14]. Alginate is a polysaccharide that is extracted from brown seaweed and is one of the gelling agents with properties such as thickening, stabilization, suspension, stabilization, gel production, viscosity, and film formation. Sodium alginate is important as a biopolymer and is widely used in medicine, pharmaceutical, industrial, water treatment sectors, the textile industry, health, and cosmetics [15–17]. Sodium alginate dissolves in water and forms high viscosity specially used for hydrogel preparation. Hydrogels are three-dimensional, flexible polymer networks capable of absorbing large amounts of water in a swollen state given a large number of hydrophilic groups [18–20]. Cross-link bonds occur physically or in combination with physicochemical interactions. However, hydrogel-type alginate exhibits weak mechanical strength. To overcome the problematic mechanical properties of alginate adsorbents and reduce the cost, a foam-type alginate adsorbent is proposed by using the freeze-drying technique which to improve the adsorption capacity of alginate, zeolite with a three-dimensional pore structure immobilized in the alginate polymer matrix.

The assembling of polymers from biological origin such as sodium alginate to zeolite minerals represents an eco-friendly alternative to commonly employed composites which can offer improved mechanical properties and better thermal stability than the pristine biopolymer, together with good biocompatibility and biodegradability properties. Introducing zeolite into alginate polymer matrix would exert the capacity of both components, reduce the cost of adsorbent, and minimize the loss of zeolite in the practical application [21]. Alginate has been applied as green adsorbents for dye and heavy metal ions removal. However, the mechanical weakness and the high cost of pure alginate significantly limit large-scale utilization of it for treating wastewater. To enhance the mechanical strength and reduce the cost, zeolites can be utilized to combine their both advantages as adsorbents. Moreover,

they are abundant, nontoxic, and of low cost and have cation exchange properties and large surface area, and thus have been used for metal ions and dyes removal. Kazemi et al. achieved to 6.14 mg/g for cationic methylene blue dye removal from aqueous solution with alginate beads impregnated with magnetic Chitosan@Zeolite nano-composite. Hong et al. represented that the prepared zeolite-alginate foam exhibited 1.5 times higher Sr adsorption efficiency than the pure alginate foam [22]. Wang et al. obtained the maximal adsorption capacity of 119.0 mg/g for Cu(II) and 160.0 mg/g for Cd(II) using alginate-based attapulgite foams as adsorbents [23]. Several probable adsorption mechanisms, including electrostatic interaction, hydrogen bonding, ion exchange, coordination, and acid–base interaction, have been proposed to understand the interactions between solid adsorbent and dye molecules in aqueous solution. The infrared spectrophotometer analysis represented different chemical interactions of adsorbate by functional group in the adsorbent responsible for adsorption process [24, 25].

Alginate utilizes as support to immobilize zeolite and minimize its loss, and zeolite uniformly disperses in the alginate Matrix. Zeolite-based polymer composites have been successfully employed for the removal of toxic contaminants from water [26, 27]. However, there is no report on the usage of ZSM-5 zeolite-based alginate composite foam for the removal of methylene blue from water. So, in this study, a zeolite-alginate foam was prepared by a freeze-drying and post-cross-linking method and then used to remove methylene blue dye from an aqueous solution. Kinetics, isotherm, swelling, and regeneration experiments, and the parameters affecting the dye adsorption process were investigated.

Materials and methods

Materials

The chemicals used in this investigation were sodium alginate (Sigma-Aldrich, molecular weight 216.121 g/mol, composed of primarily anhydro-β-D-mannuronic acid residues ≤ 5000 (cfu/g), viscosity ≥ 2000 cP, 2% (25 °C)(lit),), methylene blue (purity > 99%, Merck), zeolite ZSM-5 (Petro-Mehr, nanoparticles with average diameter ≤ 100 nm and specific surface area 6700 m^2/g), hydrochloric acid (Sam-Chun), sodium hydroxide (Arman-Sina), and calcium chloride (Merck) without further purification.

Methods of experiments

Synthesis of calcium alginate foams

For the synthesis of calcium alginate foam (Ca/ALG), at first, 100 mL of distilled water was poured into a beaker and 4 g of sodium alginate was added slowly to prepare a uniform gel. While adding the sodium alginate, the resulting solution was stirred by a mechanical stirrer at 1200 rpm for 1 h. The resulting gel was poured

into a petri dish and frozen at -80 °C for 5 h. The frame and frozen mixtures were vacuumed and dried for 24 h to remove moisture and form a porous structure. For the cross-linking reaction, the foam was immersed in a 5% weight solution of calcium chloride for 4 h, then rinsed five times using distilled water, and finally dried in an oven at 55 °C for 24 h. For the synthesis of calcium alginate/zeolite foam (Ca/ALG/ZSM-5), the mentioned trends were repeated by adding 1% weight of nano-zeolite in the initial gel preparation stage (Fig. 1).

Characterization

Fourier transform infrared spectrometer (FTIR-AVATAR) was used to investigate the functional groups. Investigation of morphological characteristics was performed by field scanning electron microscopy (FESEM-MIRA3). X-ray diffraction (XRD-PW1730) was used to identify the structural properties of particles. Measurement of the specific surface area was taken by nitrogen adsorption–desorption analysis (BET-BELSORP MINI II). The thermal stability test was carried out with the aid of the differential scanning calorimeter/thermogravimetric analysis (DSC/TGA) (model TA Q-6000). UV spectrophotometer (RAYLEIGH UV-2601) was used to determine the concentration of dye solutions.

Swelling test

In this test, 0.2 g of the adsorbents (calcium alginate and calcium alginate/zeolite 1% foams) was floated in the beakers containing distilled water and was taken out at predetermined time intervals and weighed. The weights obtained in times 5, 10, 20, 30, 40, 60, 80, 120, 240, and 1200 min were used for water absorption investigation. The swelling ratio was calculated using the formula:

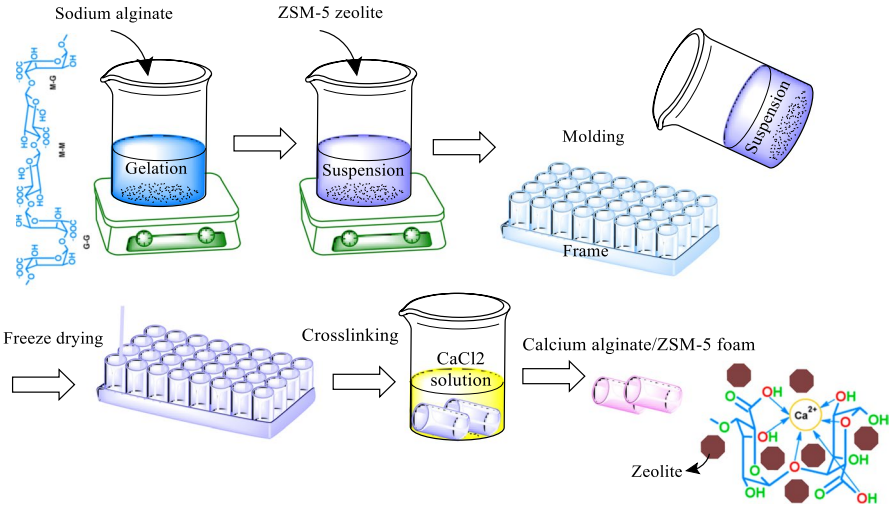

Fig. 1 Synthetic procedure of calcium alginate/zeolite foam

$$\text{Degree of swelling} = \frac{\left(W_{\text{wet}} - W_{\text{dry}}\right)}{W_{\text{dry}}} \times 100 \tag{1}$$

where W_{wet} is the wet weight and W_{dry} is the dry weight of the adsorbents.

Adsorption kinetics tests

The adsorption kinetic experiments were performed to reach the equilibrium time in the batch system. 1 g/L of the prepared adsorbents (calcium alginate and calcium alginate/zeolite 1% foams) was shacked in 10 mg/L methylene blue solution at 25 °C and 200 rpm. Sampling from the solution was performed at times 5, 10, 20, 30, 40, 60, 80, 120, 240, and 1200 min, and analyzed with UV spectrophotometer in absorption maximum at 664 nm. The dye adsorbed on the adsorbent at time t, q_t (mg/g), and equilibrium, q_e (mg/g), were determined as follows:

$$q_t = \frac{\left(C_0 - C_t\right)V}{m} \tag{2}$$

where C_0 is the initial concentration of the solution (mg/L), C_t is the concentration at time t (mg/L), V is the volume of solution (L), and m is the adsorbent mass (g). Kinetics in adsorption examines the rate and mechanism of the process. The models of pseudo-first-order, pseudo-second-order, and Elovich are common kinetic models for adsorption process investigation. The pseudo-first-order kinetic model has been widely utilized in the adsorption process description [28]. Various forms of this model are as follows [29]:

$$\frac{\mathrm{dq}_t}{\mathrm{dt}} = k_1\left(q_e - q_t\right) \tag{3}$$

$$q_t = q_e\left(1 - e^{-k_1 t}\right) \tag{4}$$

$$\ln\left(q_e - q_t\right) = -k_1 t + \ln\left(q_e\right) \tag{5}$$

Various forms of the pseudo-second-order model have been used as follows [30].

$$\frac{\mathrm{dq}_t}{\mathrm{dt}} = k_2\left(q_e - q_t\right)^2 \tag{6}$$

$$q_t = \frac{q_e^2 k_2 t}{1 + q_e k_2 t} \tag{7}$$

$$\frac{t}{q_t} = \frac{1}{q_e}t + \frac{1}{k_2 q_e^2} \tag{8}$$

In these equations, q_e and q_t are the adsorption capacity at equilibrium and any time (mg/g), respectively, k is the adsorption rate constant and t (min) is the processing time. The intraparticle diffusion kinetic model examines the mechanism of adsorption penetration into the porous adsorbent and determines the phase controlling adsorption. When the dye solution and the adsorbent are rotating, the dye molecules are transferred from the solution phase into the adsorbent pores and are considered the rate-determining step [31]. The relevant equation is as follows:

$$q_t = k_i t^{0.5} + c \tag{9}$$

In this equation, k_i is the intraparticle adsorption rate constant (mg/g $\text{min}^{0.5}$) and c is related to the thickness of the boundary layer around the adsorbent (mg/g).

The general equation of the Elovich kinetic model is as follows [32]:

$$q_t = \frac{1}{\beta}\ln(t) + \frac{1}{\beta}\ln(\alpha\beta) \tag{10}$$

Parameters α and β mean the initial adsorption rate and the area of surface coverage, respectively.

Adsorption isotherm tests

The isotherm experiment was done by making methylene blue solutions with 2, 4, 6, 8, and 10 mg/L concentration, and adding 1 g/L of the prepared adsorbents (calcium alginate and calcium alginate/zeolite 1% foams). They were then placed on a shaker at 200 rpm and at a constant temperature of 25 °C for 240 min. After that, the adsorbents were separated and the residue solution concentration was determined with a spectrophotometer.

Adsorption isotherm is a mathematical equation showing the value of the adsorptive adsorbed on the adsorbent surface in equilibrium. This means that if the adsorbent and the adsorbate are in contact at a specific and appropriate time, equilibrium is created between the adsorbate and the adsorbent, which can be described by the adsorption isotherm. The existing isotherm equation is as follows:

$$q_e = \frac{(C_0 - C_e)V}{m} \tag{11}$$

where C_e (mg/L) is the concentration at the time of equilibrium. There are several models for equilibrium distribution, including Langmuir, Freundlich, and Temkin, each of which is described below [33, 34]. The Langmuir adsorption isotherm is one of the adsorption equations proposed in 1916 by Irwin Langmuir based on the uptake of a layer of the adsorbent molecule on the adsorbent, and the adsorption bonds in this equation are reversible. The linear form of this model is as follows [35, 36]:

$$\frac{C_e}{q_e} = \frac{1}{q_m}C_e + \frac{1}{q_m K_L} \tag{12}$$

In this equation, q_m is the maximum adsorption capacity (mg/g) and K_L is the Langmuir constant (L/mg). Another adsorption isotherm model is the Freundlich equation, which was obtained experimentally and first proposed by Herbert Freundlich in 1926 [37]. In this model, the surface of the adsorbent body is assumed to be nonuniform, and thus, each part of the surface has a different adsorption power [38, 39]. The linear equation of the Freundlich model is as follows:

$$\ln\left(q_e\right) = \frac{1}{n}\ln\left(C_e\right) + \ln\left(K_F\right) \tag{13}$$

In this equation, K_F is the Freundlich constant ((mg/g)(L/mg)$^{1/n}$) and l/n is the heterogeneity factor and expresses adsorption intensity.

Temkin adsorption isotherm is another isotherm model with the linear form as follows.

$$q_e = \frac{\mathrm{RT}}{b_T}\ln\left(C_e\right) + \frac{\mathrm{RT}}{b_T}\ln\left(A_T\right) \tag{14}$$

In this equation, b_T and A_T are Temkin constants that are related to the heat and the potential of adsorption, respectively, and R is the universal constant of the gases.

Adsorbent regeneration and reuse

The regeneration of the prepared adsorbent was done in an acidic medium using a 0.2 M hydrochloric acid solution. 1 g/L of the prepared adsorbent (calcium alginate and calcium alginate/zeolite) foams was added to a 10 mg/L methylene blue solution placed on a shaker at 200 rpm at a constant temperature of 25 °C for 240 min. After that, the used adsorbent was separated from the solution and the residue concentration was determined by UV spectrophotometer, and then, adsorption capacity was calculated [40]. The separated adsorbent was immersed in the hydrochloric acid solution for 30 min. After regeneration, it was rinsed several times with distilled water and the regenerated adsorbent was used for the dye removal process again similar to the previous trends.

Effect of pH tests

10 mg/L methylene blue solutions was prepared, and the pH values were adjusted in 3, 5, 7, 9, and 11 using 0.1 M solutions of sodium hydroxide and hydrochloric acid. Then 1 g/L of calcium alginate and calcium alginate/zeolite adsorbents were added and placed on a shaker at 200 rpm for 2 h at 25 °C. Finally, the adsorbents were separated and the adsorption was investigated using the spectrophotometer.

Results and discussion

FESEM results

The investigation of the surface morphology and topography of the materials was performed with the FESEM analysis. The results related to (a-d) Ca/ALG and (e–h) Ca/ALG/ZSM-5 adsorbent with different magnifications are shown in Fig. 2. FESEM images of Ca/ALG/ZSM-5 represented a distinct change in the surface morphology that occurred when ZSM-5 zeolite was induced thoroughly on the Ca/ALG foam surface, resulting in rough and uneven surfaces.

Figures display that the foams have porous surfaces, but compared with smooth surfaces of Ca/ALG foams, the surface of Ca/ALG/ZSM-5 foam has many bumps caused by aggregation of ZSM-5, which results in surface roughness.

FTIR analysis

This analysis is used to investigate the functional groups. Figure 3 shows FTIR spectra of ZSM-5 zeolite, sodium alginate, Ca/ALG, and Ca/ALG/ZSM-5 adsorbents. In the sodium alginate FTIR spectrum, the beginning of the broad peak at 3422 cm^{-1} is related to the O–H tensile bonds and intramolecular hydrogen bonds. The peak of 2926 cm^{-1} shows the tensile bands of C-H-aliphatic groups, and the bonds of symmetric and asymmetric absorption bands of the carboxylate group are specified in the peaks of 1417 and 1615 cm^{-1}, respectively. The peak of 1031 cm^{-1} is also related to the tensile bond C-O, and the peak of 621 cm^{-1} also indicates the strong bond of C-H. In the zeolite FTIR spectrum, the peak of 800 cm^{-1} corresponds to external symmetric tension and the peak of 1097 cm^{-1} is related to internal asymmetric tensile vibrations. The crystal structure of ZSM-5 is characterized by a peak of 551 and a peak of 453 cm^{-1} showing the bending of Al-O molecules [41]. It has a very small peak at 3435 cm^{-1}, which shows that the O–H functional group within it is very low or does not exist. In the Ca/ALG FTIR spectrum, the peak 3225 cm^{-1} shows the presence of water and hydrogen bonds and belongs to the O–H factor group. The peaks 1588 and 1412 cm^{-1} are related to asymmetric and symmetric tensile vibrations of free carboxyl groups, respectively. The C–O–C tensile bond is also shown with a peak of 1016 cm^{-1}. In the Ca/ALG/ZSM-5 FTIR spectrum. According to the peak shape, 3214 cm^{-1} belongs to the O–H functional group and represents hydrogen bonding. Peaks 1595 and 1421.98 cm^{-1} indicate asymmetric and symmetric groups of carboxyl. The reason for the peak of 1070 cm^{-1} is the Al-O and Si–O bond tension in alumina silicate with zeolite structure, and the peak of 787 cm^{-1} is related to the flexural vibrations of Al–OH.

XRD analysis

The XRD analysis results are presented in Fig. 4. The materials exhibit the characteristic X-ray diffraction pattern of the ZSM-5 corresponding to the JCPDS card no. 89–1421 with the peaks at $2\theta = 13.59°$, 14.19°, 15.14°, 23.38°, 24.16°,

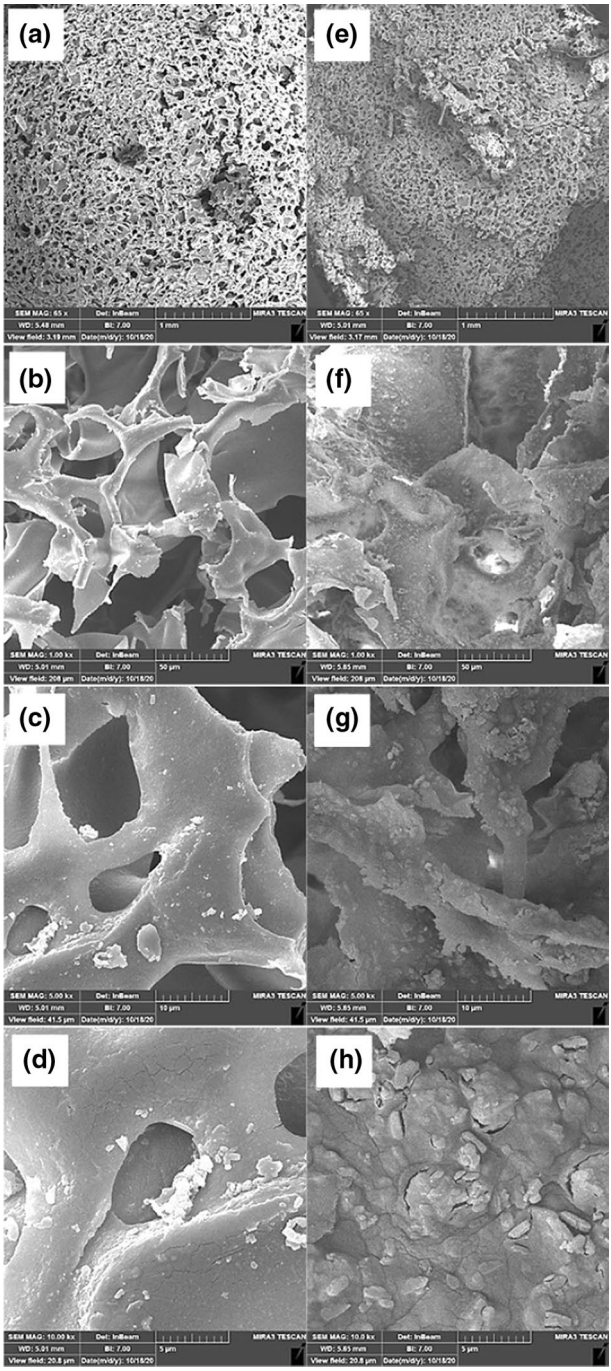

Fig. 2 FE-SEM images related to (**a**-**d**) Ca/ALG and (**e**–**h**) Ca/ALG/ZSM-5 adsorbents with different magnifications

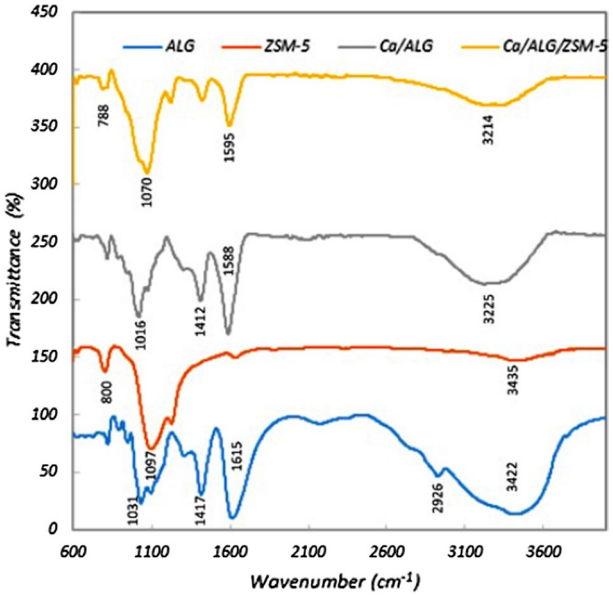

Fig. 3 FTIR spectra of sodium alginate, zeolite, calcium alginate (Ca/ALG), and calcium alginate/zeolite (Ca/ALG/ZSM-5) samples

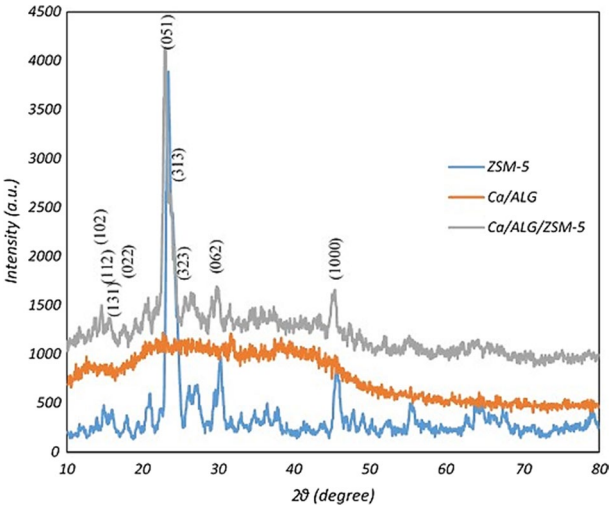

Fig. 4 Results of XRD analysis of Ca/ALG and Ca/ALG/ZSM-5 adsorbents

25.63°, 30.18°, and 45.63° that are associated with (111), (102), (112), (131), (022), (051), (313), (323), (062), and (1000) planes, respectively. A comparison of the patterns and the spectra revealed no significant shift in the location of the

characteristic peaks of the components during the preparation process of the foam, but only in their intensity.

BET analysis

The characteristics of the surface were investigated using nitrogen adsorption–desorption isotherm experiments and analyses of BET and BJH. The results presented in Fig. 5 show that the specific surface area, total pore volume, and average pore diameter of calcium alginate and calcium alginate/zeolite foams are 1.24 and 10.42 m^2/g, 0.0066 and 1.0129 cm^3/g, and 21.09 and 4.95 nm, respectively (Table1). The results shown improve the surface characteristic properties of calcium alginate with zeolite addition for adsorption. Also, both nitrogen adsorption–desorption isotherms follow the H3-type isotherm with mesoporous structures.

DSC/TGA analysis

Generally, the thermal degradation of the polysaccharides includes the absorbed water desorption, dehydration reaction, depolymerization, and, finally, the formation of aromatic and graphitic carbon structures. In the TGA results (Fig. 6), at a temperature range between 50 and 120 °C, the removal of water for foams was observed. Polymeric decomposition started at 100 and 260 °C for Ca/ALG and Ca/ALG/ZSM-5, respectively. The final decomposition of Ca/ALG and Ca/ALG/ZSM-5 was revealed at 690 and 860 °C with residue left of 6 and 33%, respectively. From the results, Ca/ALG/ZSM-5 illustrated a thermal stability improvement in comparison with Ca/ALG which can be concluded from the high thermal stability of the ZSM-5. Furthermore, in the presence of ZSM-5, the motions of the ALG networks are limited.

Kinetics study

Kinetics is one of the key parameters in measuring adsorption which depends on the physicochemical properties of the solid/solution components. The kinetic investigation was expressed using models of pseudo-first-order, pseudo-second-order, Elovich, and intraparticle diffusion, and R^2, showing the correlation coefficient, a suitable kinetic model was introduced for suggestion and use. In the pseudo-first-order model, the adsorption rate assumes directly proportional to the active sites of adsorption on the adsorbent. The model of pseudo-second-order describes the nature of bonds between adsorbate and adsorbent and the rate-determining step of the adsorption process. This was done for two samples of calcium alginate and calcium alginate/zeolite and a concentration of 5 mg/L. Figure 7a shows the diagram of C_t versus time, and Fig. 7b shows the diagram of q_t versus time. Figure 7c-e shows pseudo-first-order, pseudo-second-order, and Elovich kinetic models, respectively. Figure 7f and g shows the intraparticle diffusion model

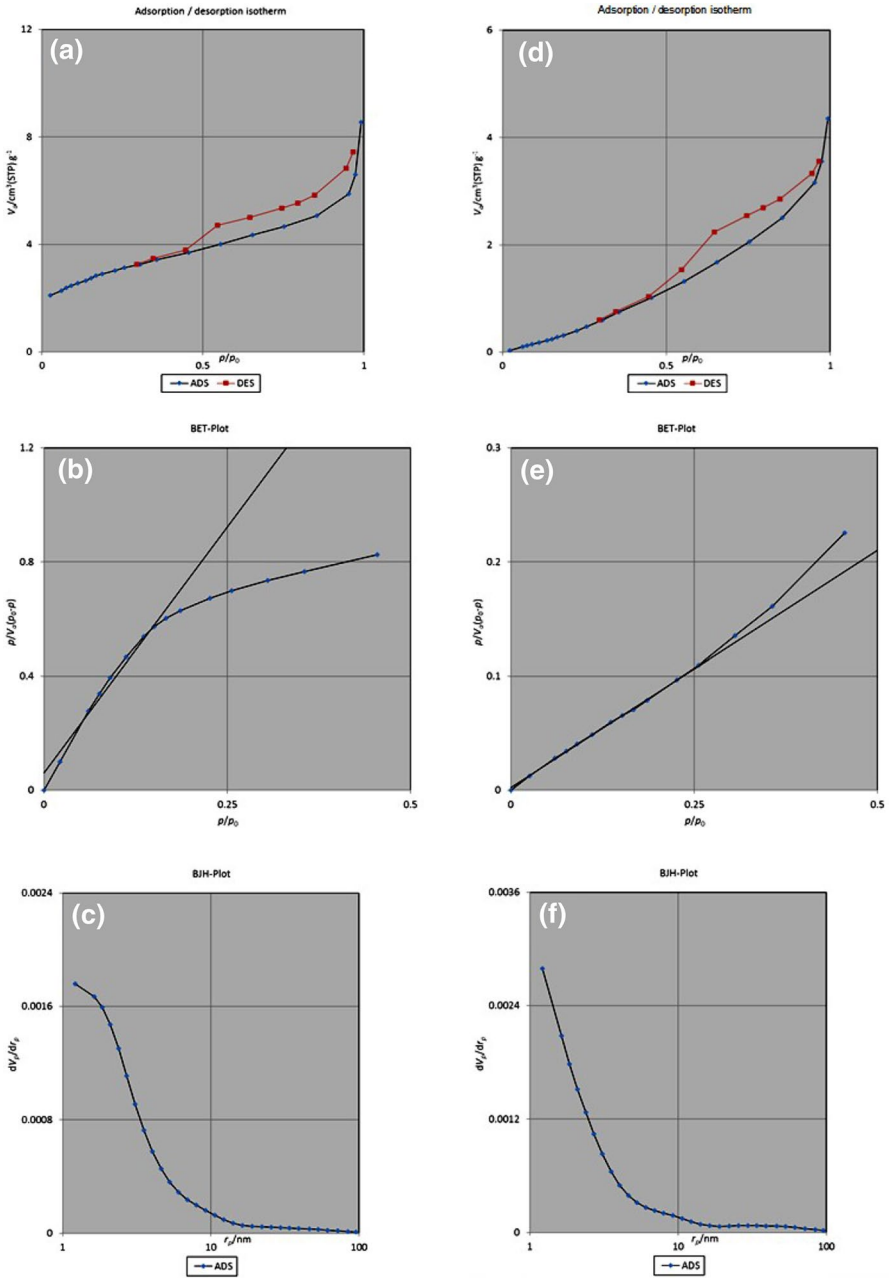

Fig. 5 Plots of (**a** and **d**) N_2 adsorption/desorption, **b** and **e** BET, and **c** and **f**) BJH results for Ca/ALG and Ca/ALG/ZSM-5 foams

Table 1 Parameters of BET plots for Ca/ALG and Ca/ALG/ZSM-5 foams

Ca/ALG	
Specific surface area ($m^2\ g^{-1}$)	1.243
Total pore volume ($cm^3\ g^{-1}$)	0.006
Average pore diameter (nm)	21.095
Ca/ALG/ZSM-5	
Specific surface area ($m^2\ g^{-1}$)	10.417
Total pore volume ($cm^3\ g^{-1}$)	0.013
Average pore diameter (nm)	4.949

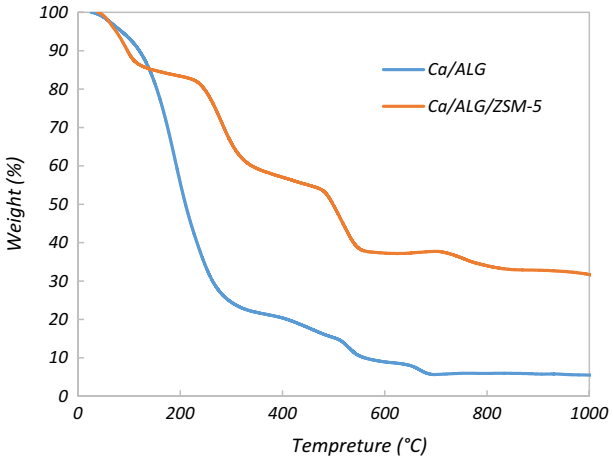

Fig. 6 Results of TGA analysis of Ca/ALG and Ca/ALG/ZSM-5 adsorbents

for Ca/ALG and Ca/ALG/ZSM-5, respectively, which show a two-step adsorption mechanism. Table 2 presents the kinetic parameters of these kinetic models.

Comparing the shapes drawn and the correlation coefficients, one can conclude that the pseudo-second-order and intraparticle diffusion models are more compatible with the adsorption process and that kinetic studies show that the adsorption rate decreases with an increase in time to the extent that the equilibrium is reached and the adsorbent is no longer able to absorb. Thus, the adsorption rate decreases after reaching equilibrium. The adsorption followed the model of pseudo-second-order with chemisorption as the rate-limiting step.

Isotherm study

Using the isotherm is useful for designing adsorption systems. Here, we examined the Langmuir, Freundlich, and Temkin isotherm models used for 25 °C. To this end, two adsorbents of Ca/ALG and Ca/ALG/ZSM-5 with 1 g/L dosage in methylene blue dye solution with concentrations of 2, 4, 6, and 8 mg/L have been used.

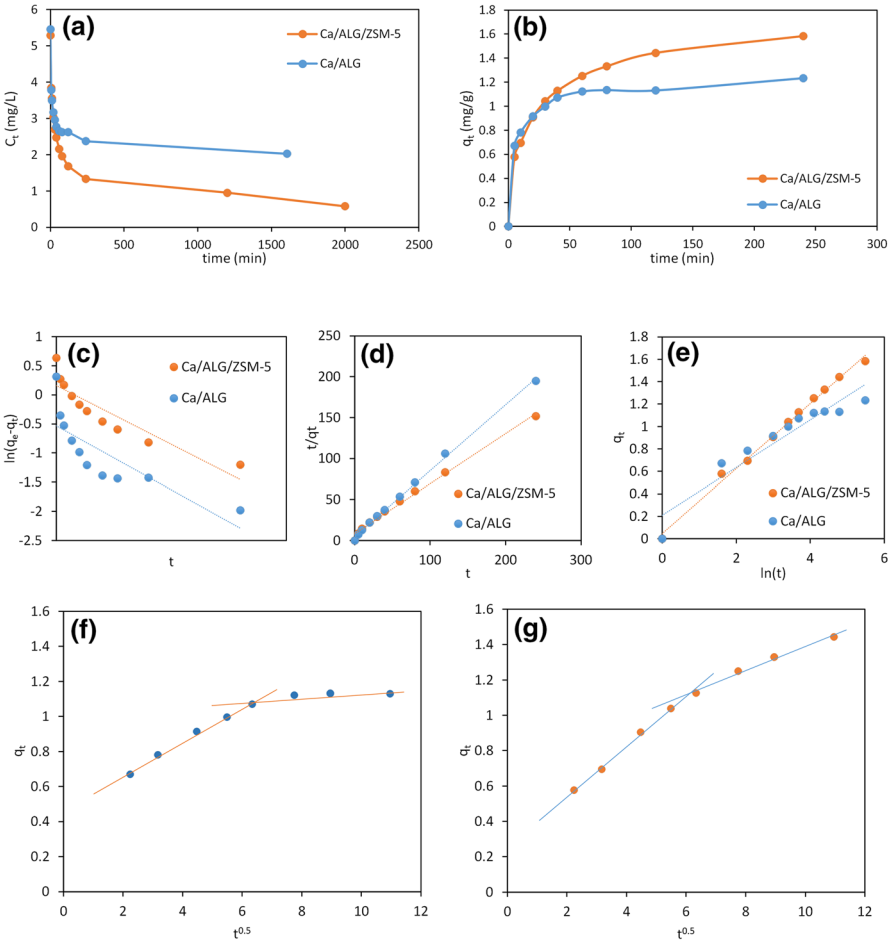

Fig. 7 **a** Diagram C_t versus time, **b** diagram of q_t versus time, **c-e** diagrams of pseudo-first-order, pseudo-second-order, and Elovich kinetic models, respectively, **f-g** diagrams of the intraparticle diffusion model for Ca/ALG and Ca/ALG/ZSM-5, respectively

Figure 8a-d shows the diagrams of the adsorption isotherm, Langmuir, Freundlich, and Temkin, respectively, and Table 3 shows the different coefficients of the Langmuir adsorption isotherm models. The correlation coefficient shows that the results obtained for the calcium alginate adsorbent are more consistent with the Temkin model and for the calcium alginate/zeolite adsorbent are more consistent with the Freundlich model. In the Freundlich model, it is assumed that the surface area energy distribution and amount of adsorption are not uniform on the adsorbent, resulting in better adsorption. In the Temkin model, it is assumed that a strong bond is established between the dye molecules and the adsorbent surface, leading to more molecules being adsorbed and thus more adsorption.

Table 2 Parameters of pseudo-first-order, pseudo-second-order, Elovich, and intraparticle diffusion kinetic models for Ca/ALG and Ca/ALG/ZSM-5

Type of adsorbent	Pseudo-first-order model		
	k_1 (1/min)	q_e (mg/g)	R^2
Ca/ALG	0.1369	1.2423	0.6562
Ca/ALG/ZSM-5	0.0453	1.6363	0.8194
Pseudo-second-order model			
	k_2 (g/mg.min)	q_e (mg/g)	R^2
Ca/ALG	0.0073	0.5848	0.9980
Ca/ALG/ZSM-5	0.0063	1.1732	0.9933
Intraparticle diffusion model			
	k_1	k_2	
Ca/ALG	0.30	0.07	
Ca/ALG/ZSM-5	0.26	0.11	
Elovich model			
	α (mg/g.min)	β (g/mg)	R^2
Ca/ALG	0.5716	4.7080	0.9059
Ca/ALG/ZSM-5	2.9370	3.4482	0.9949

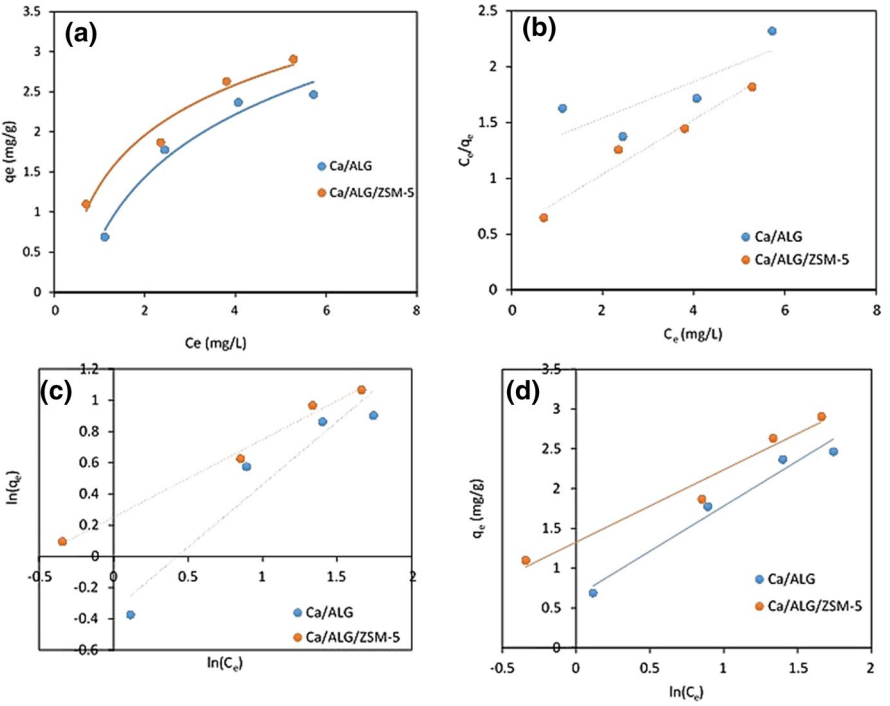

Fig. 8 **a** Diagram of the adsorption isotherm, **b** Langmuir, **c** Freundlich, and **d** Temkin models for 2, 4, 6, 8, and 10 mg/L of methylene blue, and adding 1 g/L of the prepared adsorbents (calcium alginate and calcium alginate/zeolite 1% foams) at 25 °C and 200 rpm for 2 h

Table 3 Langmuir, Freundlich, and Temkin adsorption isotherm coefficients

Type of adsorbent	Langmuir isotherm model		
	q_m	K_L	R^2
Ca/ALG	3.4650	0.4597	0.6584
Ca/ALG/ZSM-5	4.0740	0.4491	0.9652
Freundlich isotherm model			
	n	K_F	R^2
Ca/ALG	1.2434	0.7094	0.9197
Ca/ALG/ZSM-5	2.0110	1.2865	0.9905
Temkin isotherm model			
	b_T	A_T	R^2
Ca/ALG	1.1325	1.7535	0.9683
Ca/ALG/ZSM-5	0.9076	4.3253	0.9629

Study of thermodynamics of adsorption

To examine the parameters of the adsorption thermodynamics and the effect of temperature on the dye adsorption, the enthalpy (ΔH), entropy (ΔS), and Gibbs free energy (ΔG) were investigated at 298, 313, and 328 K temperatures. van't Hoff relationships were used to determine the thermodynamic parameters equations which can be expressed by Eq. (15).

$$\mathrm{Ln}\, K_d = -\frac{\Delta H}{RT} + \frac{\Delta S}{R} \tag{15}$$

where K_d ($=q_e/C_e$) T and R are the equilibrium constant at different temperatures, absolute temperature (K), and universal gas constant (8.314 mol.K^{-1}), respectively [42–44]. ΔH and ΔS determine by the slope and y-intercept of the van't Hoff plot or $\mathrm{Ln}K_d$ based on 1/T (Fig. 9). The van't Hoff diagrams were plotted and the thermodynamic parameters were obtained from them and the results are shown in Table 4. According to the results, it is revealed that the dye adsorption is exothermic (negative ΔH) and followed by entropy decrease (negative ΔS) which demonstrates the decrease of randomness at the interface between adsorbent and solution during the adsorption process.

Mechanism of the dye adsorption

The FTIR and BET of the material before and after dye removal were performed for investigated the dye adsorption mechanism. Figures 10, 11 display the FTIR and BET results of the material before and after dye adsorption, respectively. Changes in the FTIR peak frequencies or appearance and disappearance of new peaks after the adsorption process illustrates that the dye molecules are uptake to the adsorbent. As shown in Fig. 10 (FTIR analysis), it was revealed that the peaks in 1598.9 shifted to 1577.5 cm^{-1}, in 1405.9 shifted to 1400.01 cm^{-1}, and in 1012.5 shifted to 1018.3 cm^{-1}, and a change in the spectrum intensity around 3300 cm^{-1} appears

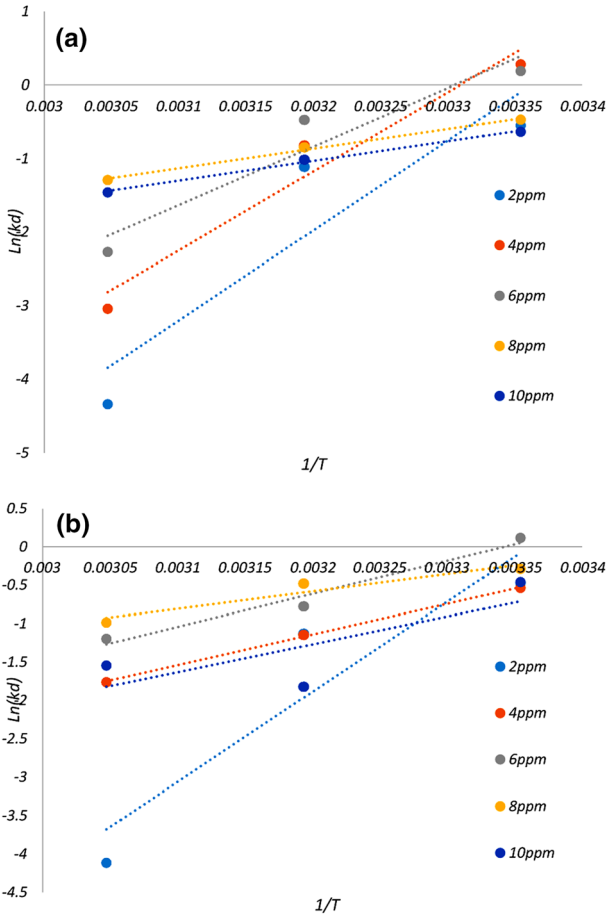

Fig. 9 Study of thermodynamics of adsorption according to van't Hoff plot for (**a**) Ca/ALG and (**b**) Ca/ALG/ZSM-5, respectively

after dye adsorption which can be due to interactions between the functional groups of the dye molecules and the hydroxyl groups of the adsorbent. On the other hand, in BET test results (Fig. 11), it is seen that the adsorption–desorption mechanism is obtained without change, but hysteresis loops have shrunk after the dye adsorption which can mean that the adsorbent pores were occupied with dye molecules.

Several probable adsorption mechanisms, including electrostatic interaction, hydrogen bonding, ion exchange, coordination, acid-base interaction, have been proposed to understand the interactions between solid adsorbent and dye molecules in aqueous solution. In the present research, as a cationic organic molecule, methylene blue could be adsorbed onto the surface of synthesized adsorbent mainly through electrostatic interaction. This can be explained by the presence of a large amount of–COOH and –OH on the adsorbent surface. As the methylene blue is aromatic molecules, aromatic alginate-based adsorbent has also been developed

Table 4 Determination of thermodynamic parameters of the dye adsorption process

Adsorbent	Conc. (mg/L)	T (K)	ΔG (kJ/mol)	ΔS (J/mol)	ΔH (kJ/mol)
Ca/ALG	2	328.15	0.579	−341.689	−101.639
		313.15	0.329		
		298.15	0.013		
Ca/ALG/ZSM-5		328.15	0.621	−327.713	−97.5149
		313.15	0.324		
		298.15	0.016		
Ca/ALG	4	328.15	1.324	−295.862	−89.4088
		313.15	0.441		
		298.15	0.048		
Ca/ALG/ZSM-5		328.15	0.585	−115.66	−33.1837
		313.15	0.318		
		298.15	0.172		
Ca/ALG	6	328.15	1.209	−218.824	−66.2085
		313.15	0.625		
		298.15	0.103		
Ca/ALG/ZSM-5		328.15	1.123	−119.489	−35.7519
		313.15	0.460		
		298.15	0.302		
Ca/ALG	8	328.15	0.626	−78.5141	−22.2932
		313.15	0.430		
		298.15	0.275		
Ca/ALG/ZSM-5		328.15	0.751	−64.869	−18.7655
		313.15	0.618		
		298.15	0.374		
Ca/ALG	10	328.15	0.531	−80.0281	−22.3306
		313.15	0.362		
		298.15	0.232		
Ca/ALG/ZSM-5		328.15	0.632	−106.78	−30.0776
		313.15	0.161		
		298.15	0.213		

based on the π-π stacking interaction. In addition, the hydrogen bond is another intermolecular interaction involved in the construction of alginate-based adsorbent, which can be easily formed between the nitrogen- or oxygen-containing groups in methylene blue and adsorbent.

The results of the parameters affecting the dye adsorption

Figure 12a shows the effect of the zeolite content used in the foam structure (1, 2, and 4%). As can be shown, the higher the amount of zeolite, the better the adsorption performance which illustrates the positive adsorptive role of the ZSM-5 zeolite in the foam. Figure 12b indicates the effect of the initial dye concentration on the adsorbent capacity for the calcium alginate and calcium alginate/zeolite adsorbents. As is shown, with an increase in the concentration, the adsorption capacity increases because the driving force related to the mass transfer increases, and thus, more

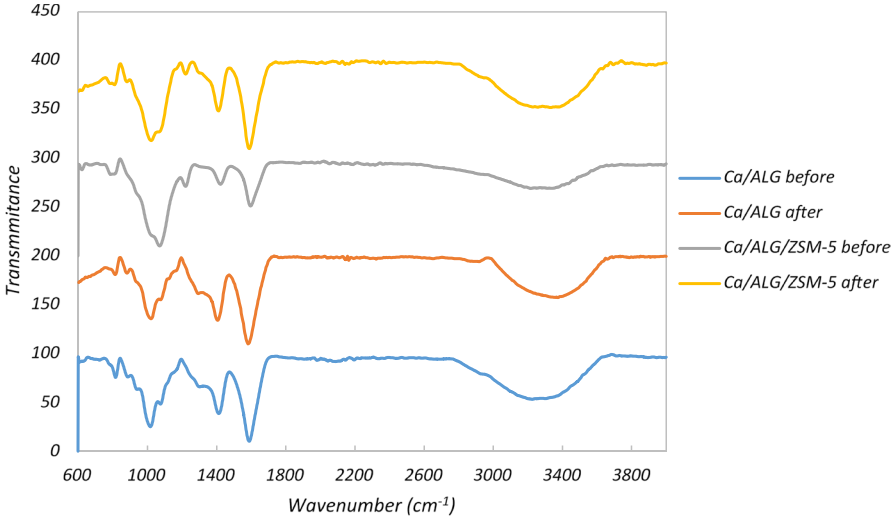

Fig. 10 FTIR results of the material before and after dye removal

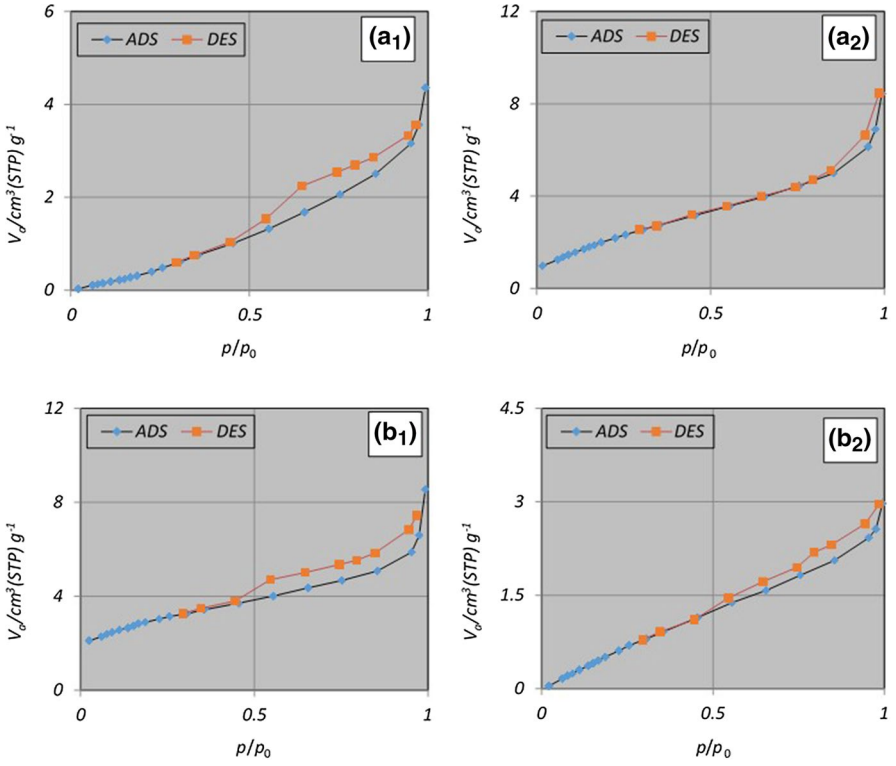

Fig. 11 BET results of the material before ((**a**1) Ca/ALG and (**b**1) Ca/ALG/ZSM-5) and after ((**a**2) Ca/ALG and (**b**2) Ca/ALG/ZSM-5) dye removal

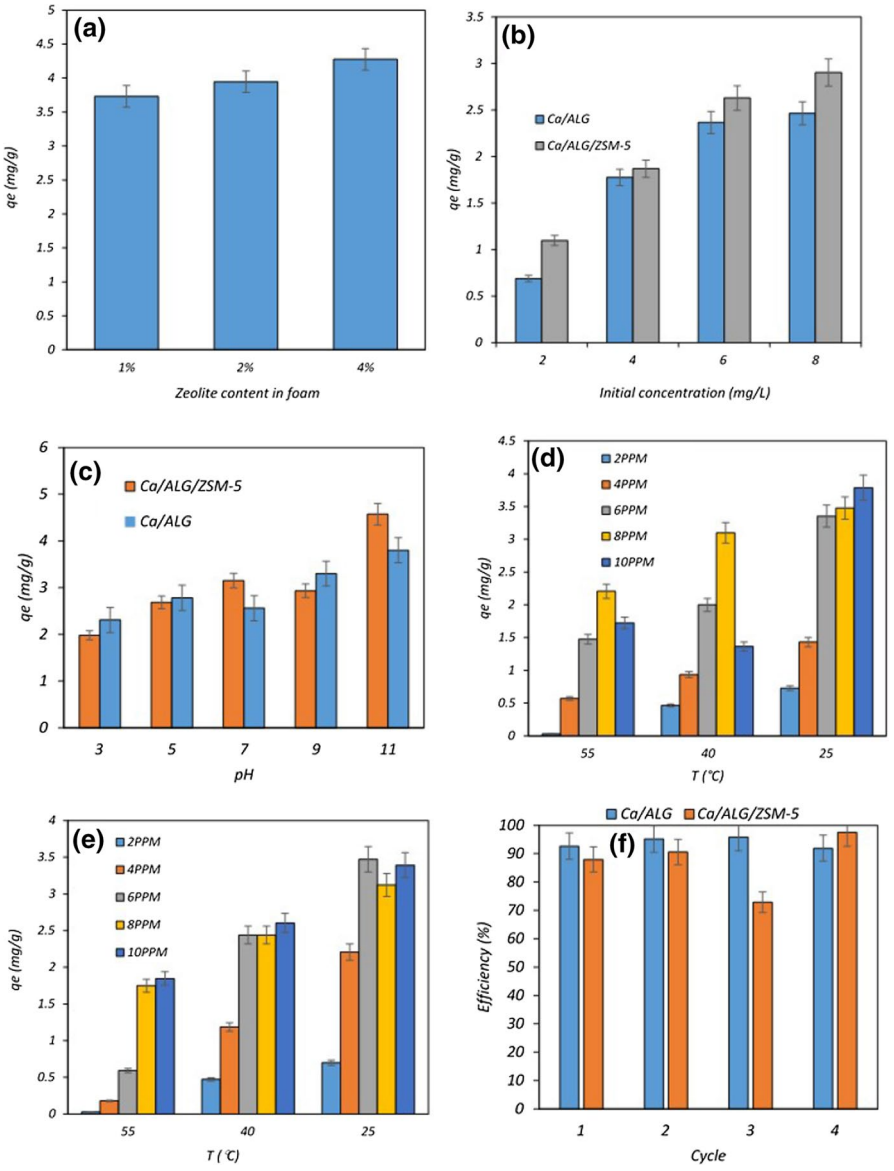

Fig. 12 Effect of (**a**) zeolite content, **b** initial concentration, **c** pH, **d**—Ca/ALG, **e**, Ca/ALG/ZSM-5) temperature on the dye adsorption, and **f** regeneration and reuse tests for the Ca/ALG and Ca/ALG/ZSM-5 adsorbents

dye can be transferred to the adsorbent surface, enhancing the adsorption capacity. It is seen that in different concentrations, the adsorption capacity of Ca/ALG/ZSM-5 is higher than Ca/ALG and the reason is the presence of zeolite improves the performance of the adsorbent. Figure 12c illustrates the effect of pH on the

adsorption performance of the Ca/ALG and Ca/ALG/ZSM-5 adsorbents. As is seen, with an increase in pH, the adsorption capacity increases. In acidic environments, the value of H^+ is high and in competition with positive cationic ions of methylene blue, it is adsorbed on the adsorbent surface and as a result, the adsorption capacity decreases. At higher pH, the value of H^+ is less and thus the competition with positive methylene blue ions for adsorption on the adsorbent surface is less, and then positive methylene blue ions are more adsorbed which increases the adsorption capacity of methylene blue. To investigate the temperature effect on the adsorption process, the tests were done at various temperatures, and Fig. 12d and Fig. 12e presents the results and that the adsorption process is exothermic which is consistent with thermodynamic results. On the other hand, with an increase in the temperature the adsorption decreases because, with temperature increases, kinetic energy is more than the electrostatic interaction between dye molecules and adsorbent which can decrease the adsorption capacity [45]. Figure 12f shows the regeneration and reusing results of the adsorbents as very important parameters in the application of the adsorbents. According to the results, after four cycles of regeneration and reuse, the adsorbents are still capable of methylene blue removal. As Fig. 13a shows, the fabricated Ca/ALG and Ca/ALG/ZSM-5 had hydrophilic nature with zero degrees contact angle. Figure 13b presents the rate of swelling ratio versus time and swelling ratio of Ca/ALG/ZSM-5 foam in comparison to that of Ca/ALG foam. On the other hand, according to swelling test results, with an increase in time, the swelling ratio of the Ca/ALG and Ca/ALG/ZSM-5 foams increased until this amount was fixed after a certain period (equilibrium). The results show both the foams exhibited a high swelling ratio, but Ca/ALG represented a higher swelling ratio than Ca/ALG/ZSM-5. By adding zeolite to the Ca/ALG structure, the swelling ratio was decreased. Immobilization of ZSM-5 zeolite in Ca/ALG caused the transformation of mesopores toward micropores (according to BET results) and resulted in a compact Ca/ALG structure with improvement in swelling resistance of the Ca/ALG/ZSM-5 and a low swelling ratio. Also, comparing the adsorption capacity of the prepared adsorbents with other similar adsorbents was performed. The results presented in Table 5 show that the adsorbents had a compatible adsorption capacity to remove methylene blue dye from aqueous solutions. On the other hand, textural wastewater is usually a mixture of different dyes. For this purpose, we performed the dye adsorption process with the presence of anionic eriochrome black T dye as a binary system of cationic (methylene blue) and anionic (eriochrome black T) dyes. The experiments were done by 0.02 g of the prepared adsorbents in 20 mL of a mixture of 10 mg/L of methylene blue and eriochrome black T dye under shaking at 200 rpm for 2 h. At the end of time, the adsorbents were removed and the residue concentration of the solution was determined using the spectrophotometer. The results represent (Fig. 13c) that the adsorbent can be able to remove both dyes especially Ca/ALG/SZM-5 adsorbent which it could be concluded that the adsorbents have removal capability of different dyes and real samples which are a mixture of different dyes.

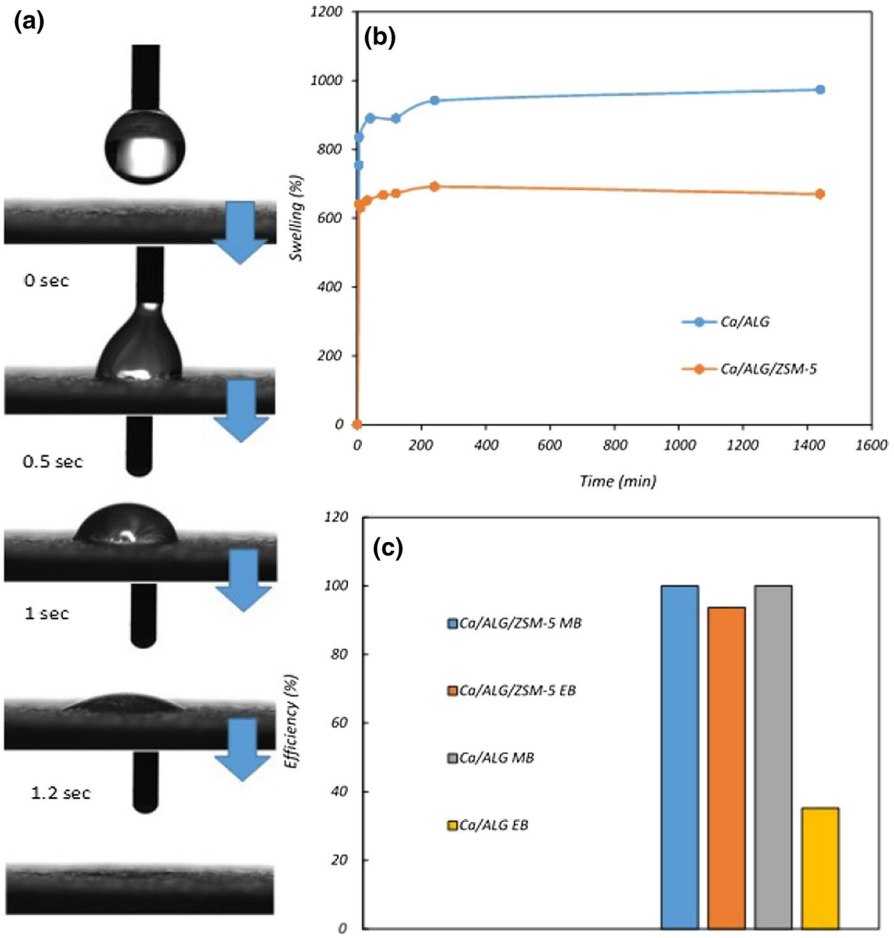

Fig. 13 **a** Dynamic contact angle photographs, (**b**) swelling investigation, and **c** binary system results for methylene blue (MB) and eriochrome black T (EB) removal for Ca/ALG and Ca/ALG/ZSM-5 adsorbents

Table 5 Comparison of the adsorption capacity of methylene blue by various adsorbents

Adsorbent	Initial concentration (mg/L)	Adsorption capacity (mg/g)	Reference
PAN-g-alginate (Alginate grafted polyacrylonitrile beads)	6	3.51	[46]
Polyurethane foam	4.8	4.27	[47]
PMMA-g-alginate	6	5.25	[48]
Ca/ALG foam	10	3.80	This study
Ca/ALG/ZSM-5 foam	10	4.57	This study

Conclusion

Alginate-based ZSM-5 zeolite foams were synthesized via simple freeze-drying and post-cross-linking method for removal of methylene blue. Kinetics, isotherm, swelling, regeneration experiments, and the parameters affecting the dye adsorption process were investigated. The results of the batch adsorption process indicated that the methylene blue adsorption using synthetic adsorbents has good conformity with conventional kinetic and isotherm models and the kinetics and isotherm are adjusted with the pseudo-second-order and the Temkin models, respectively. The adsorption capacity of methylene blue was 4.57 mg/g with 97% removal efficiency for alginate-based foam induced by ZSM-5 zeolite. With the increase in solution pH and concentration and zeolite content in the foam structure, better adsorption performance was observed. The prepared adsorbents presented remarkable chemical stability and were readily recyclable with floatability in an aqueous solution.

Acknowledgements Financial support for this work by the ACECR Institute of Higher Education (Isfahan Branch) is gratefully appreciated.

Authors' contributions Maryam Kanani was responsible for conceptualization. Vahid Javanbakht took part in writing, reviewing, and editing .

Funding Not applicable.

Data availability Not applicable.

Declarations

Conflict of interests We have no conflict of interest to declare.

Ethical Approval Not applicable.

References

1. E.M. Abd El-Monaem, A.M. Omer, R.E. Khalifa, A.S. Eltaweil, J. Col. & Int. Sci. **620**, 333 (2022)
2. Z. Hamami, V. Javanbakht, Ceramics Int. **47**(17), 241 (2021)
3. A. Miri, H.O.S. Vahed, M. Sarani, Res. Chem. Intermed **44**(11), 6907 (2018)
4. M. Mahmoodi, V. Javanbakht, Int. J. Bio. Macro. **167**, 1076 (2021)
5. N. Marsiezade, V. Javanbakht, Int. J. Bio. Macro. **162**, 1140 (2020)
6. I.K. Basha, A. El-Monaem, M. Eman, R.E. Khalifa, A.M. Omer, A.S. Eltaweil, Sci. Rep. **12**(1), 1 (2022)
7. V.K. Gupta, S. Agarwal, R. Ahmad, A. Mirza, J. Mittal, Int. J. Bio. Macro. **158**, 1310 (2020)
8. P.K. Mondal, R. Ahmad, J. Environ. Res. Dev **3**, 807 (2009)
9. A. El-Monaem, M. Eman, A.M. Omer, G.M. El-Subruiti, M.S. Mohy-Eldin and A.S. Eltaweil Bio. Con. Bio. 1 (2022)
10. A.M. Omer, E.M. Abd El-Monaem, A.S. Eltaweil, Int. J. Bio. Macro. **208**, 925 (2022)
11. M. Irandoost, M. Pezeshki-Modaress, V. Javanbakht, J. Wat. Proc. Eng. **32**, 100981 (2019)
12. Z. Sareban, V. Javanbakht Korean, J. Chem. Eng. **34**, 2886 (2017)
13. V. Javanbakht, S.M. Ghoreishi, N. Habibi, M. Javanbakht, Pro. Met. Phy. Chem. Sur. **53**(4), 693 (2017)
14. V. Javanbakht, S.M. Ghoreishi, N. Habibi, M. Javanbakht, Pow. Tech. **302**, 372 (2016)
15. A. Mirza, R. Ahmad, Gr. Sus. Dev. **11**, 100373 (2020)

16. I. Hasan, R. Ahamd, Gr. Sus. Dev. **8**, 82 (2019)
17. A.S. Eltaweil, E.M. Abd El-Monaem, H.M. Elshishini, H.G. El-Aqapa, M. Hosny, A.M. Abdelfatah, M.S. Ahmed, E.N. Hammad, G.M. El-Subruiti, M. Fawzy, RSC Adv. **12**(13), 8228 (2022)
18. M. Bayat, V. Javanbakht, J. Esmaili, Int. J. Bio. Macro. **116**, 607 (2018)
19. S.I. Mohammadabadi, V. Javanbakht, Ind. Cro. & Pro. **168**, 113575 (2021)
20. V. Javanbakht, R. Shafiei, Int. J. Bio. Macro. **152**, 990 (2020)
21. Y. Wang, Y. Feng, J. Yao, J. Col. Int. Sci. **533**, 182 (2019)
22. H.-J. Hong, B.-G. Kim, J. Ryu, I.-S. Park, K.-S. Chung, S.M. Lee, J.-B. Lee, H.S. Jeong, H. Kim, T. Ryu, J. Environ. Manage **205**, 192 (2018)
23. Y. Wang, Y. Feng, X.-F. Zhang, X. Zhang, J. Jiang, J. Yao, J. Col. Int. Sci. **514**, 190 (2018)
24. M.A. Kurniawan, N.S. Sukma and D. Ang. In: AIP Conference Proceeding (AIP Pub. LLC, 2018), p. 020093
25. I. Cosme-Torres, M. Macedo-Miranda, P. Ibarra-Escutia, M. Manjarrez-Olvera, V. Albíter-López, A. Trujillo-Segura, MRS Adv. **5**(62), 3247 (2020)
26. S. Radoor, J. Karayil, J. Parameswaranpillai, S. Siengchin, Sci. Rep. **10**, 1 (2020)
27. R. Sabarish, K. Jasila, J. Aswathy, P. Jyotishkumar and S. Suchart Int. J. Env. Sci. Tech., 1 (2020)
28. I. Langmuir, J. Am. Chem. Soc. **40**(9), 1361 (1918)
29. T.D. Reynolds and P.A.C. Richards, Unit Ope. Proc. in Env. Eng., PWS Pub. Co. (1995)
30. H. Freundlich Col. & Cap Chem. Methuen, London., 45, 797 (1926)
31. H. Freundlich, W. Heller, J. the Am. Chem Soc. **61**(8), 222 (1939)
32. M.M. Yallapu, S.F. Othman, E.T. Curtis, B.K. Gupta, M. Jaggi, S.C. Chauhan, Biomat. **32**(7), 1890 (2011)
33. J.-W. Rhim, LWT-Food Sci. Tech. **37**(3), 323 (2004)
34. S. Rahpeima, V. Javanbakht, J. Esmaili, J. Inorg. Organo. Pol. Mat. **28**(1), 195 (2018)
35. R.L. Davidson, Handbook of water-soluble gums and resins, (1980)
36. V. Javanbakht, P. Aghili Russian, J. App. Chem. **94**(5), 680 (2021)
37. J.G. Cook, Handbook of textile fibres: man-made fibres, Elsevier, (1984)
38. S. Anand and A.R. Horrocks, Handbook of technical textiles, CRC Press/Woodhead Pub. (2000)
39. M.R. Sabouri, V. Javanbakht, D.J. Ghotbabadi, M. Mehravar, Proc. Saf. Env. Prot. **126**, 182 (2019)
40. V. Javanbakht, Z. Rafiee, J. Mol. Struc. **1249**, 131552 (2022)
41. R. Aravindhan, N.N. Fathima, J.R. Rao, B.U. Nair, Col. Sur. A: Physi. Eng. Asp. **299**(1–3), 232 (2007)
42. F. Keyvani, S. Rahpeima, V. Javanbakht, Sol. Sta. Sci. **83**, 31 (2018)
43. M. Radjai, H. Ferkous, Z. Jebali, H. Majdoub, R. Bourzami, G. Raffin, M. Achour, A. Gil, M. Boutahala, J. Mol. Liq. **361**, 119670 (2022)
44. K. Noufel, N. Djebri, N. Boukhalfa, M. Boutahala, A. Dakhouche, Gro. Sus. Dev. **11**, 100477 (2020)
45. S. Sugashini, K.M.M.S. Begum, New Carb. Mat. **30**(3), 252 (2015)
46. S. Ahmed, M.S. Mohd, A.N. Ahmedy, J.K. Khairil, Der. Pharma. Chem. **7**(2), 237 (2015)
47. H.-C. Yang, J.-L. Gong, G.-M. Zeng, P. Zhang, J. Zhang, H.-Y. Liu, S.-Y. Huan, J. Col. Int. Sci. **505**, 67 (2017)
48. A. Salisu, M.M. Sanagi, K.J. Abd Karim, N. Pourmand, W.A.W. Ibr Ahim, J. Tek. **76**, 13 (2015)